

NUMERICAL STUDY OF THERMAL STREAK SPACING IN TURBULENT BOUNDARY LAYER WITH CONSTANT HEAT-FLUX BOUNDARY CONDITION

Iztok Tiselj, Elena Pogrebnyak, Albert Mosyak, Gad Hetsroni

Department of Mechanical Engineering
Technion - Israel Institute of Technology
Haifa 32000
Israel

ABSTRACT

Direct numerical simulation (DNS) of the fully developed thermal field in a flume was performed. Constant heat flux boundary condition was imposed on the heated bottom in a way, which allowed tracing of the temperature fluctuations on the wall. Free surface boundary conditions for momentum and adiabatic boundary condition for temperature were applied on the free surface. Ill-posedness of the energy equation with such boundary conditions was removed with an additional constrain: average non-dimensional wall temperature was fixed to zero.

DNS was performed at constant friction Reynolds number $Re=171$ and Prandtl numbers 1 and 5.4. The type of the boundary condition did not affect the profile of the mean temperature. The main difference between two types of boundary conditions is in the temperature RMS fluctuations, which retain a nonzero value on the wall for constant heat flux boundary condition, and zero for constant non-dimensional temperature. Certain changes are visible also in the behavior of skewness, flatness, and other turbulent statistics in the near-wall region.

An important issue is the difference between the thermal streak spacing on the isoflux wall and the velocity streak spacing near the wall. While the thermal streaks closely follow the velocity streaks for isothermality wall boundary condition, the temperature streaks near the isoflux wall do not coincide with the velocity low speed streaks. The DNS shows that thermal streak spacing near the wall depends on Prandtl number. Thermal streak spacing is larger than the velocity streak spacing and is approaching to the well known value of the velocity streak spacing (90-100 wall units) at Prandtl number $Pr=5.4$.

INTRODUCTION

Heat transfer in the turbulent boundary layer is of great importance from scientific and engineering points of view. A large number of experimental and numerical studies have been devoted to the understanding of the near-wall turbulence. In the last decade the direct numerical simulation (DNS) became an important research tool of the basic mechanisms of the near-wall turbulent heat transfer. Review of the DNS results obtained in the field of heat transfer is presented by Kasagi and Iida, 1999. They described the basic numerical methods, discussed the DNS at Prandtl numbers higher than 1.0, the DNS including

the buoyancy effects, and the application of the DNS in the area of turbulent heat transfer control.

Kim and Moin 1989, and Kasagi et al. (1992) performed one of the first direct numerical simulations of the turbulent heat transfer near the smooth wall. These simulations were performed for Prandtl numbers between 0.1 and 2.0. Recent DNS of turbulent channel heat transfer for medium Prandtl numbers were performed by Kawamura et al. (1998) using finite difference method and Na et al. (2000), while Na et al. (1999) used Lagrangian approach for the "heat markers" to simulate the heat transfer at Prandtl numbers up to 2400.

All the DNS mentioned above were using constant non-dimensional temperature boundary condition on the heated wall. The DNS assumption that the wall temperature fluctuations are zero, cannot explain the existence of the thermal pattern on the heated solid wall, placed into the turbulent flow. Such a pattern, often referred to as thermal streaks, was observed and studied in experiments carried out by Iritani et al. (1984), and Hetsroni et al. (1997). These studies showed that wall temperature fluctuations are not zero under constant wall heat flux boundary condition.

Heat transfer calculations, assuming both zero and nonzero wall temperature fluctuations, were performed by Kasagi et al. (1989) and Sommer et al. (1994). The analytical results of these studies are very useful in estimating the RMS of temperature fluctuations on the wall. These studies were performed using turbulent model and not by DNS. The thermal pattern on the wall and the existence of the thermal streaks were not discussed.

In the present paper we study numerically the turbulent transport of passive scalars in a flume by directly solving unsteady, three-dimensional Navier-Stokes equations and the energy equation for thermal field. Two types of wall boundary conditions are investigated and compared: isothermal (for non-dimensional temperature) and isoflux wall boundary condition. The resulting solutions contain detailed information on the velocity and thermal fields at Prandtl number 1.0 and 5.4. Time averaged statistics, as well as turbulent structures associated with the temperature field are presented. The wall layer structures identified by the temperature field are compared for two types of boundary conditions. The role of the organized turbulent structures in heat transfer at different Prandtl numbers is discussed.

MATHEMATICAL MODEL AND NUMERICAL METHOD

The flume geometry, coordinate system and boundary conditions are shown in Fig. 1. Basic equations solved in the flume are:

$$\frac{\partial u_j}{\partial x_j} = 0 \quad (1)$$

$$\frac{\partial u_i}{\partial t} = -\frac{\partial u_i u_j}{\partial x_j} + \nu \nabla^2 u_i - \frac{1}{\rho} \frac{\partial p}{\partial x_i} \quad (2)$$

$$\frac{\partial T}{\partial t} = -\frac{\partial T u_j}{\partial x_j} + \alpha \nabla^2 T \quad (3)$$

Bottom wall of the flume is heated with a constant heat flux, while top surface of the flume is adiabatic free surface with boundary condition for wall-normal velocity $w_{FREE_SURFACE} = 0$. Velocity boundary condition at the free surface does not take into consideration surface waves. However, experiments of Hetsroni et. al. (1997, 1999) and DNS results (Li et. al. 1999) show that this is an acceptable approximation at low Reynolds numbers, where surface waves are negligible and do not affect near wall behavior. Periodic boundary conditions are used in streamwise and spanwise directions. Temperature in Eq. (3) is treated as a passive scalar.

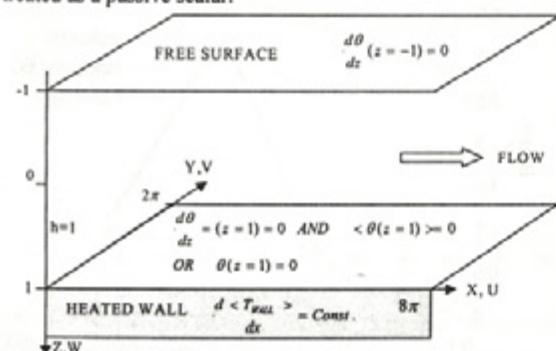


FIG 1: Flow geometry with boundary conditions.

Equations are solved with pseudo-spectral scheme using Fourier series in x and y directions and Chebyshev polynomials in wall-normal z direction. Numerical procedure and code of Gavrilakis et. al. (1986), modified by Lam and Banerjee (1988, 1989) was used to solve the continuity and momentum equation. Code was upgraded with the nondimensional energy equation

$$\frac{\partial \theta}{\partial t} = -\frac{\partial \theta u_j}{\partial x_j} + \frac{1}{Re \cdot Pr} \nabla^2 \theta + \frac{u}{2u_b} \quad (4)$$

derived by Kasagi (1992) with dimensionless temperature

$$\theta(x, y, z, t) = (\langle T_{WALL} \rangle - T(x, y, z, t)) / T_r, \quad (5)$$

which is periodic in the streamwise direction (unlike the temperature T).

Two types of approximation affect DNS of the heat transfer with Eq. (4). Prandtl number and viscosity are not constant but are the functions of temperature. Experiments of Hetsroni et. al. (1997, 1999) for example, are performed at bulk water temperature of approx. 20°C where the Prandtl number is

$Pr=7.1$, while the Prandtl number at the near-wall fluid temperature around 30°C is $Pr=5.4$. More accurate mathematical model should take into account temperature dependence of the Prandtl number and viscosity. That would introduce a new nonlinearity into equations, which could not be simply treated with the pseudospectral approach and was not taken into account in the present work. The other approximation - neglected buoyancy - is less important.

The DNS code was rewritten in order to take the advantage of the parallel computer SGI Origin 2000. The original dealiasing in the code was replaced by a more efficient one: chopping of the upper one third of the frequencies in each direction was abandoned and nonlinear terms were computed in the physical space on 1.5 times finer grid in each direction.

First version of the upgraded code was written for the constant non-dimensional temperature boundary condition $\theta=0$. Another modification was needed to implement a constant heat flux boundary condition. The problem of the ideal isoflux wall boundary condition is ill-posedness of the energy equation discussed by Sommer et. al. 1994. The ill-posedness can be quickly uncovered, if one attempts to solve the laminar form of the Equations (1), (2), (3) with constant heat flux at the wall and adiabatic free surface. The ill-posedness is removed if an additional constrain is imposed on the heated wall: time and space averaged non-dimensional wall temperature is fixed to zero $\langle \theta_{WALL} \rangle_{t,x,y} = 0$.

In the applied pseudo-spectral scheme (see Lam 1989 for details) the wall boundary condition is implemented in the last step of the algorithm, where the temperature is found as a solution of the differential equation of Helmholtz type

$$\left(\frac{d^2}{dz^2} - \frac{1 + \alpha k^2}{a} \right) \theta = H(z) \quad (6)$$

This equation with $\alpha = \Delta t / (2 Re \cdot Pr)$, $k = \sqrt{k_x^2 + k_y^2}$, and $H(z)$ containing nonlinear terms and contribution of the old time step, is solved in the wall-normal (Chebyshev) direction for each pair of wave numbers (k_x, k_y) . Boundary condition at the free surface at $z=-1$ is $d\theta/dz=0$. The isothermal boundary condition at the wall $z=1$ is $\theta=0$. For isoflux boundary condition at the wall the Eq. (4) is solved with the boundary conditions:

$$\begin{aligned} \theta(z=1) &= 0 & \text{for } k_x = k_y = 0 \\ \frac{d\theta}{dz}(z=1) &= 0 & \text{for all other pairs of } k_x, k_y \end{aligned} \quad (7)$$

Such boundary condition fixes the average wall temperature (which corresponds to the zero wave number) to zero, and at the same time allows free fluctuations of the other temperature components.

Simulations were performed for $Re_\tau = 171$ on the turbulent box of the size 2148*537*171 wall units (in computer code units: $8\pi * 2\pi * 2$) on grids with 128*64*65 and 256*128*129 collocation points in x , y and z (wall-normal) direction for $Pr=1.0$ and $Pr=5.4$ respectively. Resolution of the current simulations at $Pr=1.0$ is similar to the resolution 2356*942*300 wall units at 128x128x96 collocation points used in DNS of Kasagi et. al. (1992) for $Re_\tau = 150$ and $Pr=0.71$. (Due to the different scaling in the computer code some caution is needed when present DNS is compared with other DNS that are performed in the channels bounded by two walls. For example: half of the Kasagi's computational box in the computer code

units $5\pi * 2\pi * 1$ is equivalent to the box $10\pi * 4\pi * 2$ in the present work.) Approximately two times finer resolution in the DNS is required at $Pr=5.4$, as the smallest scales in the temperature turbulent fluctuations are known to be proportional to the $1/Pr^{1/2}$ (Tennekes, Lumley, 1972). All the turbulence statistics were calculated as an average over non-dimensional time interval $12 u_r / (2h)$ (30000 and 60000 time steps on grids $128 * 64 * 65$ and $256 * 128 * 129$ respectively).

The size of the turbulent box was chosen on the basis of the DNS performed on larger boxes: $12\pi * 4\pi * 2$ and $8\pi * 4\pi * 2$. The criterion for an acceptable box was prediction of the two-point autocorrelation functions of velocities and temperatures shown in Figs. 8 to 11 for streamwise and spanwise direction. Accurate auto-correlation functions in spanwise direction were required, since their first minimums were used for the estimation of the thermal and velocity streak half-spacing. Jimenez and Moin (1991) determined the minimal turbulent box for the flow in the channels that still gave an accurate first order statistics. Turbulent box sufficient for accurate first order statistics can be much smaller than the box used in this work, however such box is not applicable when auto-correlation functions are needed. An example of successful DNS in smaller turbulent box, which gave an accurate prediction of first order turbulence statistics, are calculations performed by Kawamura et. al. (1998) at $Re_r = 180$ and Prandtl numbers up to 5.0. Kawamura et. al. used similar resolution in wall-normal direction and approximately two times finer resolution in streamwise and spanwise directions than the present study. However, they used a finite difference scheme, which according to Moin and Mahesh (1998) requires roughly two times finer resolution than the spectral schemes for the same problem. The DNS in the box of $1074 * 537 * 171$ wall units ($4\pi * 2\pi * 2$) - similar to the one used by Kawamura et. al. (1998) - was also tested in the present work, and it gave an accurate first order turbulent statistics but was not useful for the prediction of the auto-correlation functions.

DNS RESULTS - $Pr=1$

The average non-dimensional temperature profile and temperature RMS profile near the smooth wall are shown for $Pr=1$ in Figs 2 and 3 together with results of the Kawamura's DNS (1998) at slightly different Reynolds number $Re_r = 180$ and at the same Prandtl number $Pr=1$. Results for isothermal θ on wall are almost identical to the results of Kawamura for both parameters. Minor difference is visible in θ_{RMS} profile near the free surface, since the Kawamura's results are from the channel flow bounded by two heated walls. Similar agreement between Kawamura's DNS and the isothermal θ_{WALL} is seen also in Figs. 4 to 7 where streamwise and wall-normal turbulent fluxes and cross-correlation functions between velocity and temperature are shown. Differences near the free surface are again a consequence of different boundary conditions and do not affect the near wall behavior. The same agreement between Kawamura's DNS and present DNS with isothermal θ boundary condition was achieved also for the other first-order temperature and velocity statistics, which are not presented in this work.

Verification of the auto-correlation functions of velocity and temperature was not possible with the results of Kawamura et. al. (1998) due to the small turbulent box, which did not allow Kawamura et. al. to accurately calculate the autocorrelation

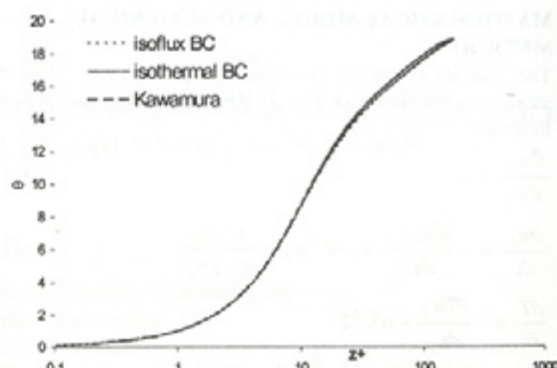


FIG2: Dimensionless temperature profile for smooth wall - DNS with constant temperature and constant heat flux performed for $Re_r = 171$, $Pr=1$, grid $128 * 64 * 65$, flume dimensions $2148 * 537 * 171$ wall units in x , y and z directions respectively. DNS of Kawamura: $Re_r = 180$, $Pr=1.0$, channel $1152 * 576 * 360$ wall units (two heated walls), resolution $256 * 256 * 128$, second-order consistent finite difference.

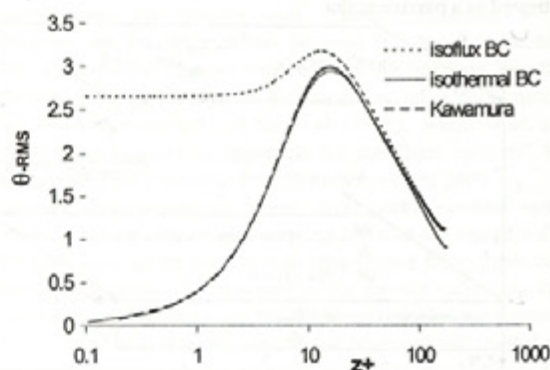


FIG 3: Dimensionless temperature RMS profile for smooth wall at $Pr=1$ - DNS with constant wall temperature θ and constant heat flux.

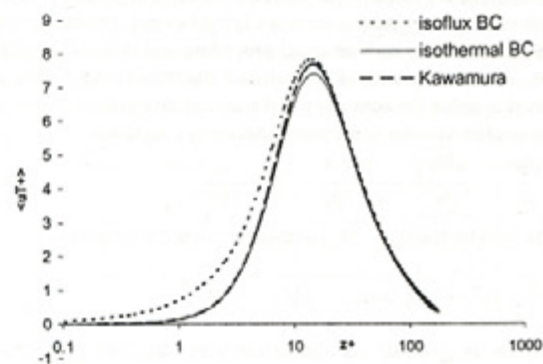


FIG 4: Streamwise turbulent heat flux ($Pr=1$).

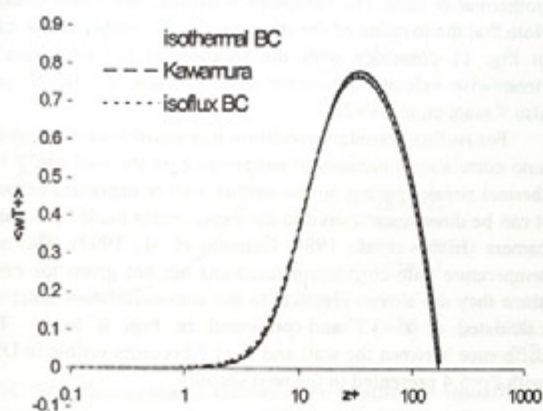


FIG 5: Wall-normal turbulent heat flux ($Pr=1$).

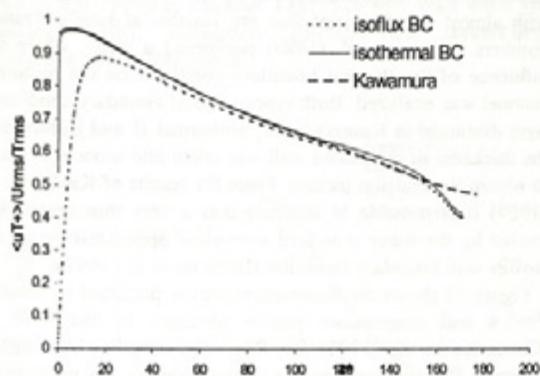


FIG 6: Cross-correlation function between streamwise velocity and temperature ($Pr=1$).

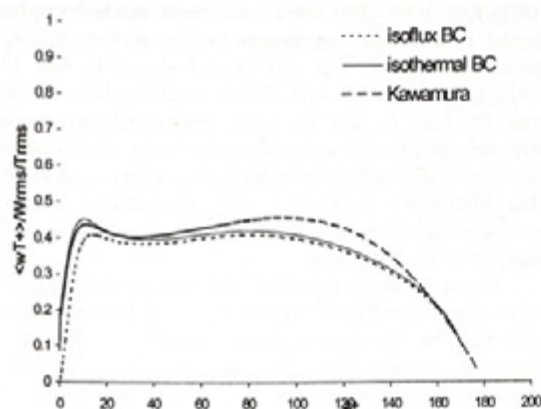


FIG 7: Cross-correlation function between wall-normal velocity and temperature ($Pr=1$).

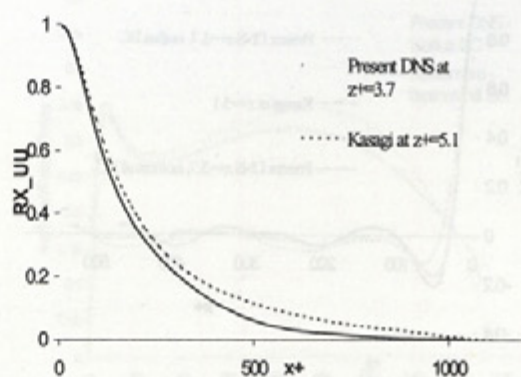


FIG 8: Auto-correlation function of streamwise velocity in streamwise direction at $z^+=3.7$ ($Pr=1$). Isoflux θ DNS was performed in three different turbulent boxes in order to find an optimal box. Kasagi's DNS (1992): $Re_\tau = 150$, $Pr=0.71$, box $2356 \times 942 \times 300$ wall units, grid $128 \times 128 \times 97$, auto-correlation calculated at $z^+=5.1$.

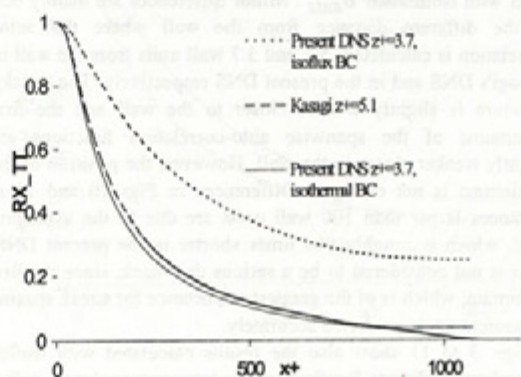


FIG 9: Auto-correlation function of temperature in streamwise direction at $z^+=3.7$ ($Pr=1$).

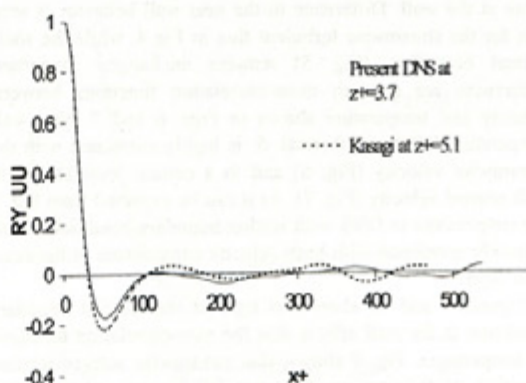


FIG 10: Auto-correlation function of streamwise velocity in spanwise direction at $z^+=3.7$ ($Pr=1$).

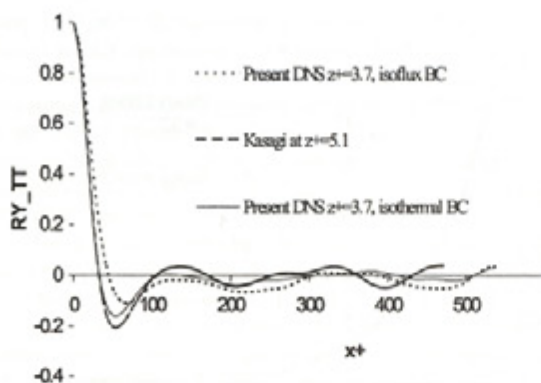


FIG 11: Auto-correlation function of temperature in spanwise direction at $z^+=3.7$ ($Pr=1$).

functions. Thus the Kasagi's DNS results (1992) at $Re_\tau = 150$ and $Pr=0.71$ are used for comparison, which is shown in Figs. 8 to 11. Kasagi's auto-correlation functions are very similar to the auto-correlation functions of the present DNS with isothermal θ_{WALL} . Minor differences are mainly due to the different distance from the wall where the auto-correlation is calculated: 5.1 and 3.7 wall units from the wall in Kasagi's DNS and in the present DNS respectively. The streaky structure is slightly weaker closer to the wall and the first minimums of the spanwise auto-correlation functions are slightly weaker closer to the wall. However, the position of the minimums is not changed. Differences in Figs 10 and 11 at distances larger than 100 wall units are due to the averaging time, which is roughly two times shorter in the present DNS. This is not considered to be a serious drawback, since the first minimum, which is of the greatest importance for streak spacing measurement, is predicted accurately.

Figs. 3 to 11 show also the results calculated with isoflux boundary conditions for θ . Average temperature shown in Fig. 2 is not affected by the type of the boundary condition. The main difference is shown in Fig. 3, where temperature RMS fluctuations for the isoflux boundary conditions retain a nonzero value at the wall. Difference in the near-wall behavior is seen also for the streamwise turbulent flux in Fig 4, while the wall-normal heat flux (Fig. 5) remains unchanged. Important differences are seen in cross-correlation functions between velocity and temperature shown in Figs. 6 and 7. Near-wall temperature for the isothermal θ is highly correlated with the streamwise velocity (Fig. 6) and to a certain level also with wall-normal velocity (Fig. 7). As it can be expected from Fig. 3 the temperature in DNS with isoflux boundary condition for θ is poorly correlated with both velocity components in the near-wall layer.

Figs 9 and 11 show that type of the thermal boundary condition at the wall affects also the auto-correlation functions of temperature. Fig. 9 shows, that streamwise auto-correlation function of temperature does not fall to zero when isoflux boundary condition is applied at the wall. Spanwise auto-correlation function of temperature shown in Fig. 11 points to an interesting phenomena - location of the first minimum, which measures the half-spacing of the thermal streaks at $z^+=3.7$ is approximately 30% larger than the location of the minimum of

isothermal θ case. The minimum in isoflux case is also weaker. Note that the location of the minimum in the isothermal θ case in Fig. 11 coincides with the location of the minimum in streamwise velocity auto-correlation function in Fig. 10 (see also Kasagi et. al. 1992).

For isoflux boundary condition it is possible to evaluate the auto-correlation functions of temperature on the wall itself. The thermal streak spacing on the isoflux wall is important because it can be directly compared to the experiments made by infrared camera (Iritani et. al., 1984, Hetsroni et. al., 1997). The wall temperature auto-correlation functions are not given for $Pr=1$, since they are almost identical to the auto-correlation functions calculated at $z^+=3.7$ and presented in Figs 8 to 11. The difference between the wall and $z^+=3.7$ becomes visible in DNS with $Pr=5.4$ presented in the next section.

DNS RESULTS - $Pr=5.4$

The DNS at $Pr=5.4$ and isoflux wall boundary condition is more important from the practical point of view, because experiments with almost constant heat flux are feasible at similar Prandtl numbers. Kasagi et. al. (1989) performed a study, where the influence of the thermal boundary condition on the turbulent channel was analyzed. Both types of ideal boundary conditions were discussed in Kasagi's work, isothermal θ and isoflux, and the thickness of the heated wall was taken into account in order to obtain the realistic picture. From the results of Kasagi et. al. (1989) it is possible to estimate that a very thin heated foil cooled by the water is indeed very close approximation of the isoflux wall boundary condition (Hetsroni et. al., 1997).

Figure 12 shows the temperature profile predicted by DNS at $Pr=5.4$ and temperature profile obtained by the DNS of Kawamura et. al. (1998) for $Re_\tau = 180$ and $Pr=5.0$. Slightly different Prandtl numbers are responsible for the differences. Figure 13 shows the profile of the temperature RMS fluctuations for DNS with isoflux boundary condition and the same parameter of Kawamura et. al. (1998) for $Re_\tau = 180$ and $Pr=5.0$. Kasagi et. al. (1989) also calculated the temperature RMS at the isoflux wall. For $Pr=7$ they obtained value $(\theta_{RMS}^*)_{WALL} = 5.8$. This value is too small, due to the turbulent model used in the calculations. Value of the $(\theta_{RMS}^*)_{WALL}$ predicted by DNS with $Pr=5.4$ and shown in Fig. 13 is $(\theta_{RMS}^*)_{WALL} = 7.5$, thus at $Pr=7.0$ the value should be between 9 and 10. Figs 14 and 15 show cross-correlation functions between velocity and temperature and show similar behavior like Figs. 6 and 7 where the same functions are plotted for $Pr=1$. The difference is thickness of the near-wall layer where the cross-correlation functions are growing: at higher Prandtl number the layer is thinner.

Figure 16 shows the streamwise auto-correlation function of temperature at $Pr=5.4$. The falling is the slowest at the wall and faster as the distance from the wall is increasing. The spanwise auto-correlation functions are plotted in Fig. 17. Location of the minimum for streamwise velocity auto-correlation at $z^+=3.7$ is 50 wall units, minimum for temperature auto-correlation at $z^+=3.7$ is slightly larger than 50 wall units and minimum for temperature auto-correlation at the wall is at approximately 55 wall units. For Prandtl number 5.4 the thermal streak spacing on the wall is thus approximately 10% higher than the spacing of the low-speed streaks in the same flow.

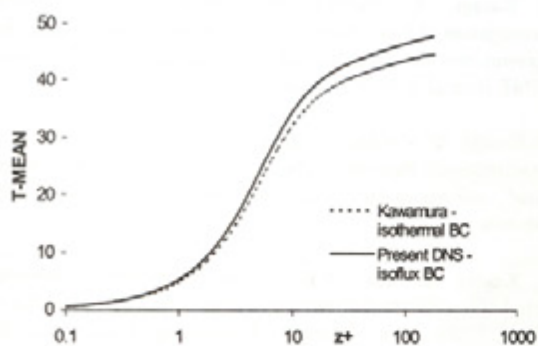


FIG 12: Dimensionless temperature profile for smooth wall - DNS with constant heat flux performed for $Re_{\tau} = 171$, $Pr = 5.4$, grid $256 \times 128 \times 129$, flume dimensions $2148 \times 537 \times 171$ wall units in x , y and z directions respectively. DNS of Kawamura with isothermal θ boundary condition: $Re_{\tau} = 180$, $Pr = 5.0$, channel $1152 \times 576 \times 360$ wall units (two heated walls), resolution $256 \times 256 \times 128$, second-order consistent finite difference.

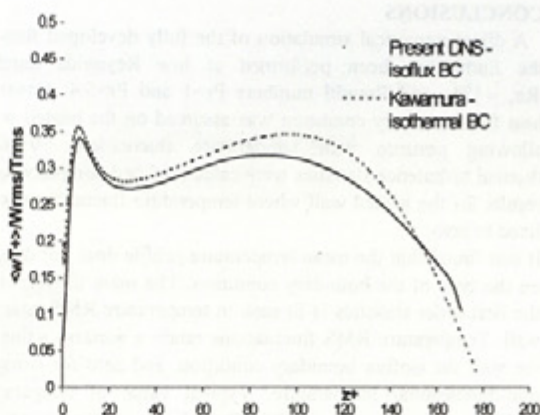


FIG 15: Cross-correlation function between wall-normal velocity and temperature ($Pr = 5.4$, Kawamura: $Pr = 5.0$).

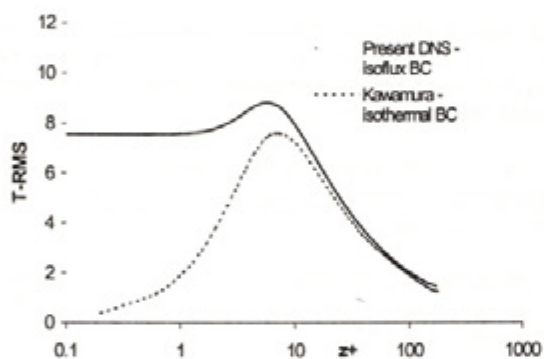


FIG 13: Dimensionless temperature RMS profile: DNS with constant heat flux at $Pr = 5.4$ and DNS of Kawamura at $Pr = 5.0$ with constant wall temperature θ .

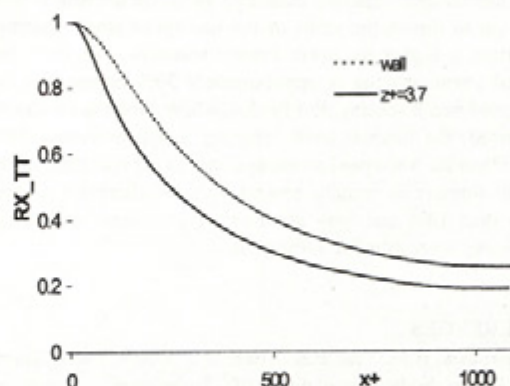


FIG 16: Auto-correlation function of temperature in streamwise direction at the wall and at $z^+ = 3.7$ ($Pr = 5.4$).

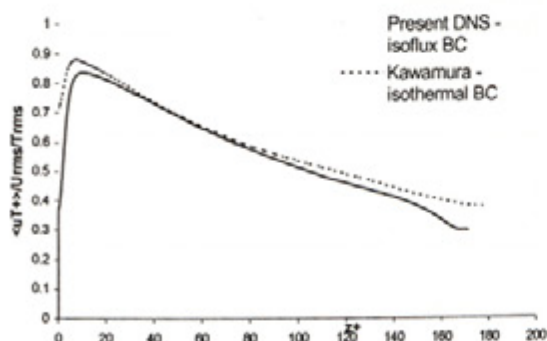


FIG 14: Cross-correlation function between streamwise velocity and temperature ($Pr = 5.4$, Kawamura $Pr = 5.0$).

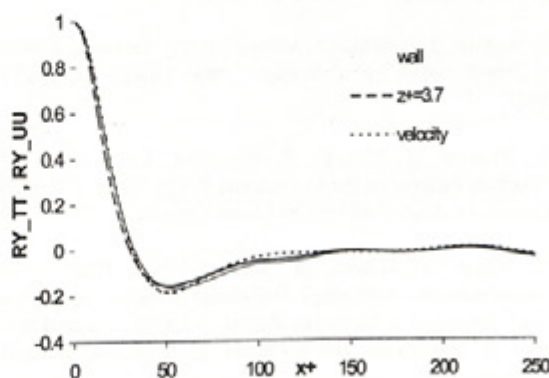


FIG 17: Auto-correlation function of temperature and streamwise velocity in spanwise direction at the wall and at $z^+ = 3.7$ ($Pr = 5.4$).

CONCLUSIONS

A direct numerical simulation of the fully developed flow in the flume has been performed at low Reynolds number $Re_\tau = 171$, and Prandtl numbers $Pr=1$ and $Pr=5.4$. Constant heat flux boundary condition was assumed on the heated wall, allowing nonzero wall temperature fluctuations. Various thermal turbulence statistics were calculated and compared with results for the heated wall where temperature fluctuations were fixed to zero.

It was found that the mean temperature profile does not depend on the type of the boundary condition. The main difference in the first order statistics is in seen in temperature RMS near the wall. Temperature RMS fluctuations retain a nonzero value on the wall for isoflux boundary condition, and zero for constant non-dimensional temperature. Typical value of temperature RMS fluctuations on the wall for $Pr=5.4$, where experiments are feasible, is about 7.5.

The size of the computational box in the DNS was chosen on the basis of the spanwise auto-correlation functions of streamwise velocity. The requirement was accurate prediction of the low-speed streak half-spacing.

Thermal streak spacing measured by the on the isoflux wall turns out to distort the value of the low-speed streak spacing. Distortion is higher for lower Prandtl numbers - for $Pr=1$, the thermal streak spacing is approximately 30% higher than the low-speed streak spacing. For $Pr=5.4$, where experiments can be performed, the thermal streak spacing is approximately 10% higher than the low-speed streak spacing. In experiments, where Prandtl number is usually around 7, this difference is even lower than 10% and very accurate measurements and image processing are required to measure it.

REFERENCES

- S. Gavrilakis, H.M. Tsai, P.R. Voke, D.C. Leslie, 1986, "Direct and Large Eddy Simulation of Turbulence", Notes on Numerical Fluid Mechanics 15, ed. U. Schumann, R. Friedrich, Vieweg, Braunschweig, D.B.R., 105.
- G. Hetsroni, R. Rozenblit, D. M. Lu, 1995, "Heat Transfer Enhancement by a Particle on the Bottom of a Flume", Int. Journal of Multiphase Flow 21, 963-984.
- G. Hetsroni, J. L. Zakin, A. Mosyak, 1997, "Low-speed Streaks in Drag-Reduced Turbulent Flow", Phys. Fluids, Vol. 9, 2397-2404.
- G. Hetsroni, A. Mosyak, R. Rozenblit, L.P. Yarin, 1999, "Thermal Patterns on the Smooth and Rough Walls in Turbulent Flows", Int. Journal of Heat and Mass Transfer 42, 3815-3829.
- Y. Iritani, N. Kasagi, M. Hizata, 1983, "Heat Transfer Mechanism and Associated Turbulence Structure in the Near-Wall Region of a Turbulent Boundary Layer", Proceedings of the 4th Symposium on Turbulent Shear Flows, Karlsruhe, Germany.
- J. Jimenez, P. Moin, 1991, "The Minimal Flow Unit in Near-Wall Turbulence", Journal of Fluid Mechanics 225, 213-240.
- N. Kasagi, A. Kuroda, M. Hirata, 1989, "Numerical Investigation of Near-Wall Turbulent Heat Transfer Taking Into Account the Unsteady Heat Conduction in the Solid Wall", ASME Journal of Heat Transfer 111, 385-392.
- N. Kasagi, Y. Tomita, A. Kuroda, 1992, "Direct Numerical Simulation of Passive Scalar Field in a Turbulent Channel Flow", Journal of Heat Transfer, Transactions of ASME 114, 598-606.
- N. Kasagi, O. Iida, 1999, "Progress in Direct Numerical Simulation of Turbulent Heat Transfer", Proceedings of the 5th ASME/JSME Joint Thermal Engineering Conference, San Diego.
- H. Kawamura, K. Ohsaka, H. Abe, K. Yamamoto, 1998, "DNS of Turbulent Heat Transfer in Channel Flow with low to medium-high Prandtl number fluid", Int. Journal of Heat and Fluid Flow 19, 482-491.
- J. Kim, P. Moin, 1989, "Transport of Passive Scalars in a Turbulent Channel Flow", in: Turbulent Shear Flows VI, Springer-Verlag, Berlin, pp. 85-96.
- K.L. Lam, S. Banerjee, 1988, "Investigation of Turbulent Flow Bounded by a Wall and a Free Surface", Fundamentals of Gas-Liquid Flows, Edited by Michaelides, Sharma, Vol. 72, 29-38, ASME, Washington DC.
- K.L. Lam, 1989, "Numerical Investigation of Turbulent Flow Bounded by a Wall and a Free-Slip Surface", Ph.D. Thesis, Univ. Calif. Santa Barbara.
- P. Moin, K. Mahesh, 1998, "Direct Numerical Simulation: A Tool in Turbulence Research", Annual Review of Fluid Mechanics 30, 539-578.
- Y. Na, D.V. Papavassiliou, T.J. Hanratty, 1999, "Use of Direct Numerical Simulation to Study the Effect of Prandtl Number on Temperature Fields", Int. Journal of Heat and Fluid Flow 20, 187-195.
- Y. Na, T.J. Hanratty, 2000, "Limiting Behavior of Turbulent Scalar Transport Close to a Wall", Int. Journal of Heat and Mass Transfer 43, 1749-1758.
- C. R. Smith, J. D. A. Walker, 1995, "Turbulent Wall-Layer Vortices", in Fluid Vortices, 235-290, Kluwer Academic Publishers.
- T.P. Sommer, R.M.C. So, H.S. Zhang, 1994, "Heat Transfer Modeling and the Assumption of Zero Wall Temperature Fluctuations", ASME Journal of Heat Transfer 116, 855-863.
- H. Tennekes, J.L. Lumley, 1972, "A First Course in Turbulence", MIT Press, Cambridge, MA.